Determination of the forward Compton

scattering amplitudes for C and Pb

A. Deppman[*], N. Bianchi, E. De Sanctis[†],

M. Mirazita, V. Muccifora, P. Rossi

Laboratori Nazionali di Frascati,

Istituto Nazionale di Fisica Nucleare,

P.O.Box 13, 00044 Frascati (Roma), Italy.

February 9, 2008

Abstract

The forward Compton scattering amplitudes for carbon and lead have been calculated from total photoabsorption cross section data by using dispersion relations. The results show a large difference between the scattering amplitudes for nuclei and the free nucleon, above the Δ region. Difference

---

[†]DESANCTIS@LNF.INFN.IT

between carbon and lead is also evident. The forward Compton scattering cross sections have been calculated and compared with the available data. The Weise sum rule is discussed together with the predictions of a recent theoretical model.

PACS: 14.20.Gk, 21.60.-n, 25.20.Dc

Keywords: photoabsorption, dispersive relation, Compton scattering.

1   Introduction

Intermediate energy photonuclear reactions have been intensively studied in the last few years to investigate the nucleon's properties in nuclear matter. In this context, the spin averaged Forward Compton scattering Amplitude (FCA) is an interesting quantity, since it is directly related to the scattered wave function and to the scattering potential. In addition, it allows to connect photon-nucleon and photon-nucleus cross sections through a generalized photoabsorption sum rule which reconciles the enhancement of the low-energy integrated photonuclear cross section over the classical dipole sum with the shadowing behaviour observed at high-energy.

In 1988, Ahrens et al. [1] performed a dispersion relation analysis of the photoabsorption cross section. Due to the lack of nuclear data at intermediate energies (from about 0.5 to about 2 GeV), their analysis was accurate to energies up to the Δ resonance region. They found that the real part of the nuclear FCA

has a universal zero at the photon energy $\omega = 327 \pm 5$ MeV throughout the periodic table, and close to the zero for the free proton, found at $\omega = 318$ MeV. This fact was interpreted as a clear evidence that the Δ-resonance survives as a quasi-particle in nuclei with mass shifted by only a small amount from the free Δ-resonance mass. On the contrary recent measurement of the total photoabsorption cross sections for several nuclei in the energy region 300-1200 MeV has shown that the Δ-resonance mass and width increase almost linearly with the nuclear density [2].

The topic of the hadronic mass modifications in the nuclear medium has received intense interest of the theoretical community. For a review see reference [3]. In particular, it is worth noticing that the nuclear medium dependence of the baryon mass implies a change in the properties of the vacuum which translates into a scaling (density and/or temperature dependence) of the free model paramenters. In this context recently Mukhopadhyay and Vento [4] have analysed the baryon and meson mass shifts in nuclei in the framework of two different QCD-inspired models, offering for the first time different insights and connections in a subject well known in the traditional nuclear physics domain. In particular their investigation has shown that the baryon mass shift suggests a partial quark deconfinement in the nuclear medium.

Recently, Boffi et al. [5] used the Weise sum rule [6] to check the consistency of the model they proposed for describing the resonance broadening and shadowing effect in the nuclear photoabsorption. Their finding is that above 1 GeV a region

should exist where impulse approximation is valid, i.e. the Compton amplitudes for free and bound nucleons are the same. In addition, because of the influence of nucleon correlations, they predicted a small anti-shadowing effect at photon energies below 2 GeV, where no photoabsorption data were available at the time.

Given the new photonuclear data in the intermediate energy region [7, 2], the total photoabsorption cross section is now well known for a series of nuclei at photon energies up to about 80 GeV. This allows an accurate dispersion relation analysis over the nucleonic resonances and shadowing threshold energy regions. In this paper this analysis is performed for carbon, lead, proton and neutron from $\omega = 0.14$ to $\omega = 5$ GeV. In section 2 we give the formalism used in the analysis, in section 3 we describe the procedure for the calculation of the FCAs, in section 4 and 5 we present and discuss the results for the FCA and the forward Compton scattering cross section, and in section 6 we recall the major findings.

2 Formalism

2.1 The Forward Scattering Amplitudes

The imaginary part of the FCA, $f_{\gamma,A}$, for photon scattering on a nucleus of mass number A is related to the nuclear total photoabsorption cross section, $\sigma_{\gamma,A}$, through the optical theorem

$$Im f_{\gamma,A}(\omega) = \frac{\omega}{4\pi}\sigma_{\gamma,A}(\omega)\,. \tag{1}$$

4

Once the $\sigma_{\gamma,A}(\omega)$ is known for all energies, the real part of the FCA can be calculated by using the Kramers-Kronig relation and the well known Thomson limit [6]

$$Ref_{\gamma,A}(\omega) = -\frac{1}{2\pi^2}\frac{Z^2}{A}S + \frac{\omega^2}{2\pi^2}P\int_0^\infty \frac{\sigma_{\gamma,A}(\omega')d\omega'}{\omega'^2 - \omega^2}, \qquad (2)$$

where Z is the number of protons in the target, $S = \frac{2\pi^2 e^2}{m} = 60$ GeV μb is the value for the classical dipole sum, m is the nucleon mass, and P denotes the principal value of the integral.

For energies above the pion photoproduction threshold, μ, it is useful to isolate in Eq. 2 the contribution below μ [6] :

$$Ref_{\gamma,A}(\omega) = -\frac{1}{2\pi^2}\frac{Z^2}{A}S + \frac{\omega^2}{2\pi^2}\int_0^\mu \frac{\sigma_{\gamma,A}(\omega')d\omega'}{\omega'^2 - \omega^2} + \frac{\omega^2}{2\pi^2}P\int_\mu^\infty \frac{\sigma_{\gamma,A}(\omega')d\omega'}{\omega'^2 - \omega^2}, \qquad (3)$$

and, using the Taylor expansion of the second term on the right-hand side,

$$Ref_{\gamma,A}(\omega) \cong -\frac{1}{2\pi^2}\frac{Z^2}{A}S - \Sigma_\mu + \delta(\omega) + \frac{\omega^2}{2\pi^2}P\int_\mu^\infty \frac{\sigma_{\gamma,A}(\omega')d\omega'}{\omega'^2 - \omega^2}, \qquad (4)$$

where

$$\Sigma_\mu = \frac{1}{2\pi^2}\int_0^\mu \sigma_{\gamma,A}(\omega')d\omega' \qquad (5)$$

and

$$\delta(\omega) = \frac{-1}{2\pi^2}\int_0^\mu \left(\frac{\omega'}{\omega}\right)^2 \sigma_{\gamma,A}(\omega')d\omega' \qquad (6)$$

are the first and third terms in the Taylor expansion. The $\delta(\omega)$ term, which

5

main contribution comes from the quasi-deuteron region ($\omega = 80 - 140$ MeV), is small compared to Σ_μ [8, 9, 10]. In this energy range and for all nuclei, $\frac{1}{A}\sigma_{\gamma,A}(\omega) < \frac{1}{A}\sigma_{\gamma,A}^{max} = 200$ μb then one can write:

$$|\delta(\omega)| < |\delta_{max}(\omega)| = |-\frac{\sigma_{\gamma,A}^{max}}{6\pi^2 A}\frac{\mu^3}{\omega^2}| = 3.38\frac{\mu^3}{\omega^2}GeV\mu b \qquad (7)$$

which is low for $\omega >> \mu$. In the following calculation we assumed $\delta = 0$ in Equation 4, and evaluated the upper limit of the relevant error due to this approximation by using the relation 7.

2.2   The Weise sum rule

Using the dispersion relation in Equation 4 for the nucleon and for the nucleus, Weise derived the following sum rule [6]:

$$\int_0^\mu d\omega\sigma_{\gamma A}(\omega) = \frac{NZ}{A}S[1 + \zeta(A, Z)], \qquad (8)$$

where

$$\zeta(A, Z) = \frac{A}{NZ}\left\{5\frac{R(\omega_0) + I(\omega_0)}{S} + \left[\frac{A_{eff}(\omega_0)}{A} - 1\right]Z\right\}, \qquad (9)$$

$$R(\omega_0) = 2\pi^2[A_{eff}(\omega_0)Ref_{\gamma,N}(\omega_0) - Ref_{\gamma,A}(\omega_0)], \qquad (10)$$

$$I(\omega_0) = \omega_0^2\int_\mu^\infty d\omega\frac{A_{eff}(\omega_0) - A_{eff}(\omega)}{\omega_0^2 - \omega^2}\sigma_{\gamma N}(\omega), \qquad (11)$$

6

$A_{eff} = \sigma_{\gamma A}/\sigma_{\gamma N}$ is the effective number of nucleons participating in the photon-nucleus interaction, ω_0 is an energy at our disposal, large compared to the pion threshold μ, the free nucleon FCA $f_{\gamma,N}(\omega)$, and the photon-nucleon cross section $\sigma_{\gamma,N}(\omega)$, are defined as an average over the numbers of protons and neutrons in the nucleus:

$$f_{\gamma,N}(\omega) = \frac{Z}{A} f_{\gamma,p}(\omega) + \frac{N}{A} f_{\gamma,n}(\omega), \tag{12}$$

$$\sigma_{\gamma,N}(\omega) = \frac{Z}{A} \sigma_{\gamma,p}(\omega) + \frac{N}{A} \sigma_{\gamma,n}(\omega). \tag{13}$$

3 Calculation procedure

We performed the calculation of the real part of the FCA of Equation 4 by using the experimental values of Σ_μ (specifically: 1.91 NZ/A for carbon and 1.75 NZ/A for lead [8, 9, 10]) and fits to the whole set of available data [7, 2, 11, 12, 13] for the numerical integration of the high energy integral.

As a fitting expression we used the sum of a resonance and a background contributions, were the latter includes all non-resonant processes. Here, our main interest has not been focoused on the extraction of the resonance parameters, but only on the determination of the most faithfull mathematical description of the data.

The resonance contribution for the nucleon and the nuclei has been parametrized

by a superposition of Breit-Wigner shapes [14]

$$\sigma_{res}(s) = \sum_{i=1}^{6} \sigma_i \frac{M_i^2 \Gamma_i^2}{(s - M_i^2)^2 + M_i \Gamma_i^2} \, , \tag{14}$$

where $\Gamma_i = \Gamma_i^0 (\frac{k}{k_r})^{2j_i}$; $s = 2m\omega + m^2$; σ_i, M_i and Γ_i^0 are free parameters; k and k_r are the center of mass photon momenta at the energy ω and at the resonance peak energy, respectively; and j_i is the photon total angular momentum. The index i refers to the six resonances considered in the fits, specifically: the P_{33}, D_{13}, F_{15}, P_{11}, F_{37}, S_{11}.

For the nucleon and for photon energies ω up to 4 GeV, we calculated the background contribution with the expression

$$\sigma_{back}^{p(n)}(\omega) = (b_1^{p(n)} + \frac{b_2^{p(n)}}{\sqrt{\omega}})\{1 - exp[-2(\omega - \mu)]\} \, , \tag{15}$$

where the indexes p and n refer to the proton and neutron, and the constants are $b_1^p = 91$ μb, $b_2^p = 71.4$ μb GeV$^{1/2}$, $b_1^n = 87$ μb, $b_2^n = 65$ μb GeV$^{1/2}$ [15]. Above 4 GeV we fitted the cross sections to the following expression, which is known to provide a good Regge behaviour [16]

$$\sigma_{back}^{p(n)}(\omega) = X^{p(n)} s^{0.0808} + Y^{p(n)} s^{-0.4525} \, , \tag{16}$$

with $X^{p(n)}$ and $Y^{p(n)}$ free parameters.

For the nuclei, we calculated the background contribution with the expression

$$\sigma_{back}^A(\omega) = \frac{Z}{A}\sigma_{back}^p(\omega) + \frac{N}{A}\sigma_{back}^n(\omega)\,. \qquad (17)$$

To this, we added a coherent contribution, σ_c, through the quasi-deuteron model:

$$\sigma_c(\omega) = L\frac{NZ}{A}\sigma_{\gamma d \to np}(\omega), \qquad (18)$$

with the deuteron photodisintegration cross section, $\sigma_{\gamma d \to np}(\omega)$, calculated by using the fit of Rossi et al. [17], and the Levinger constant values L given by Tavares et al. [18]. In addition, to include the shadowing effect, we multiplied the cross section for nuclei by the factor

$$h(\omega) = 1 - K_1 exp(-K_2/\omega^2) - K_3 exp(-K_4/\omega^2)\,, \qquad (19)$$

with the constants K_i (i = 1,4), different for each nucleus, being free parameters in the fit.

In Figure 1 we compare the fits with the data: the reduced χ^2 are 0.37, 0.13, 0.4 and 0.22 for C, Pb, p and n, respectively. The data for proton are from reference [12], those for carbon and lead are the total photo-hadronic cross sections from the HEPDATA compilation [13] and from references [7, 2]. The data for the neutron were obtained from the deuteron ones [12] by using the procedure described in references [2, 19].
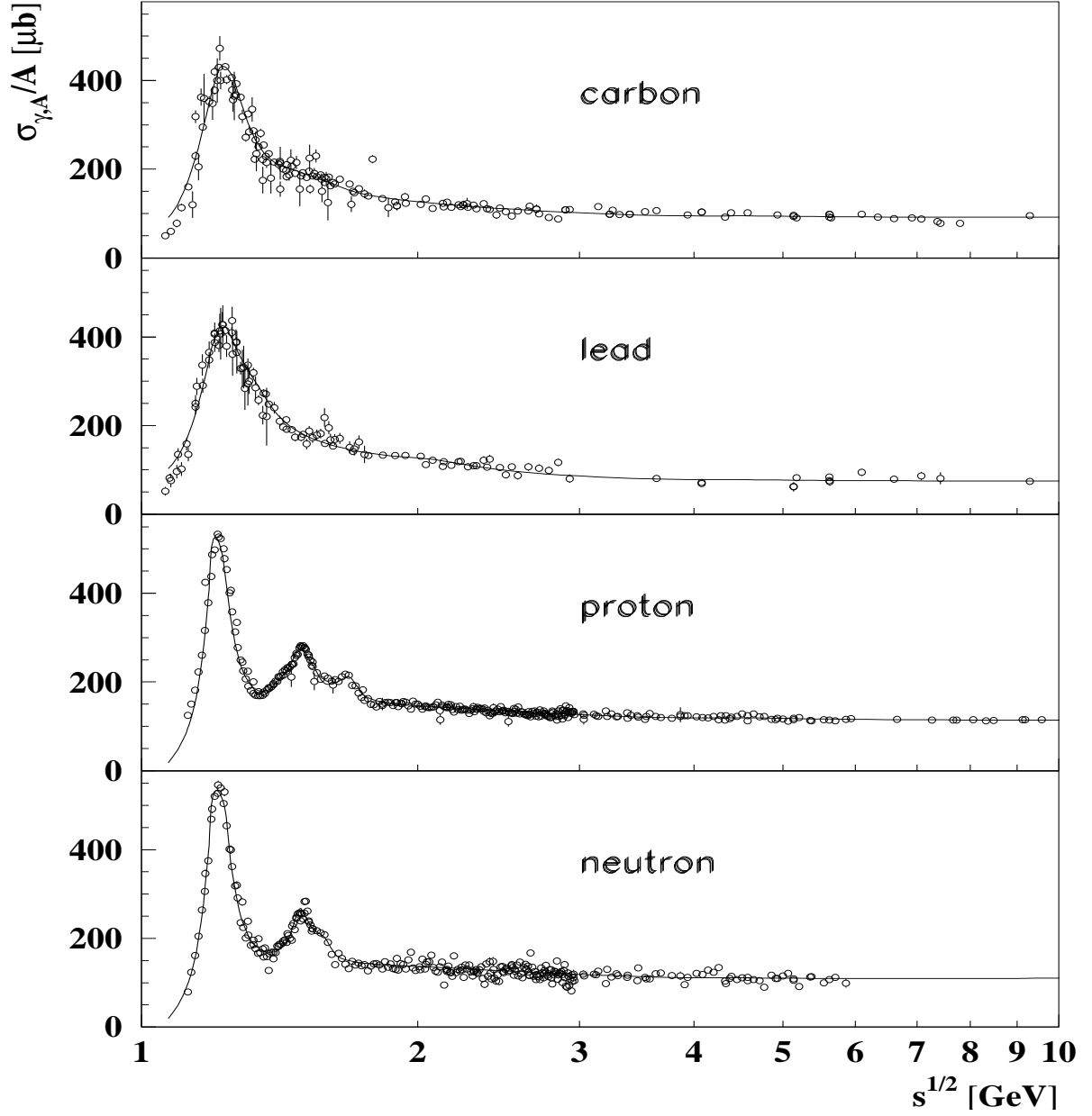
Figure 1: Data for the total photoabsorption cross section and the relevant fits used in the calculation of the FCA for the given nuclei .

4 The forward Compton amplitudes

The real and imaginary parts of the FCA were calculated from Equations (1) and (4) by numerical integration of the fits to the photoabsorption cross sections. The results are shown in Fig. 2. In order to give an estimate of the error due to the approximation $\delta = 0$ used in Eq. 4, the quantity $\delta_{max}(\omega)$ is also shown in the Figure. As it is seen, $|\delta_{max}(\omega)| < 0.1 \ GeV\mu$b for $\omega > 0.3$ GeV and therefore the used approximation is reliable above that energy. For the sake of comparison with the free-nucleon, the nuclear FCAs have been divided by the relevant mass numbers. Henceforth the shortned form FCA expresses this quantity.

Both the real and the imaginary FCA curves for the free-nucleon and for the nuclei have similar shapes in the Δ-resonance region, reflecting clearly the Δ-resonance excitation in the nucleus. The different Δ-resonance width, which is more clearly seen in the $Imf(\omega)$ curves, is due to Fermi motion and to Δ-resonance propagation in nuclear matter.

On the contrary, above the Δ-resonance region and up to $\omega \simeq 1.2$ GeV, they are quite different: while the signatures of the high-mass nucleon resonances are evident in the curves for the free-nucleon, they are absent in those for nuclei. This difference can not be attributed to the smearing due to the integration over the Fermi momentum only [20]. Moreover, the absolute values of the real and imaginary FCA curves for the bound-nucleon are significantly lower than those for the free-nucleon. The latter effect persists at higher energies where the
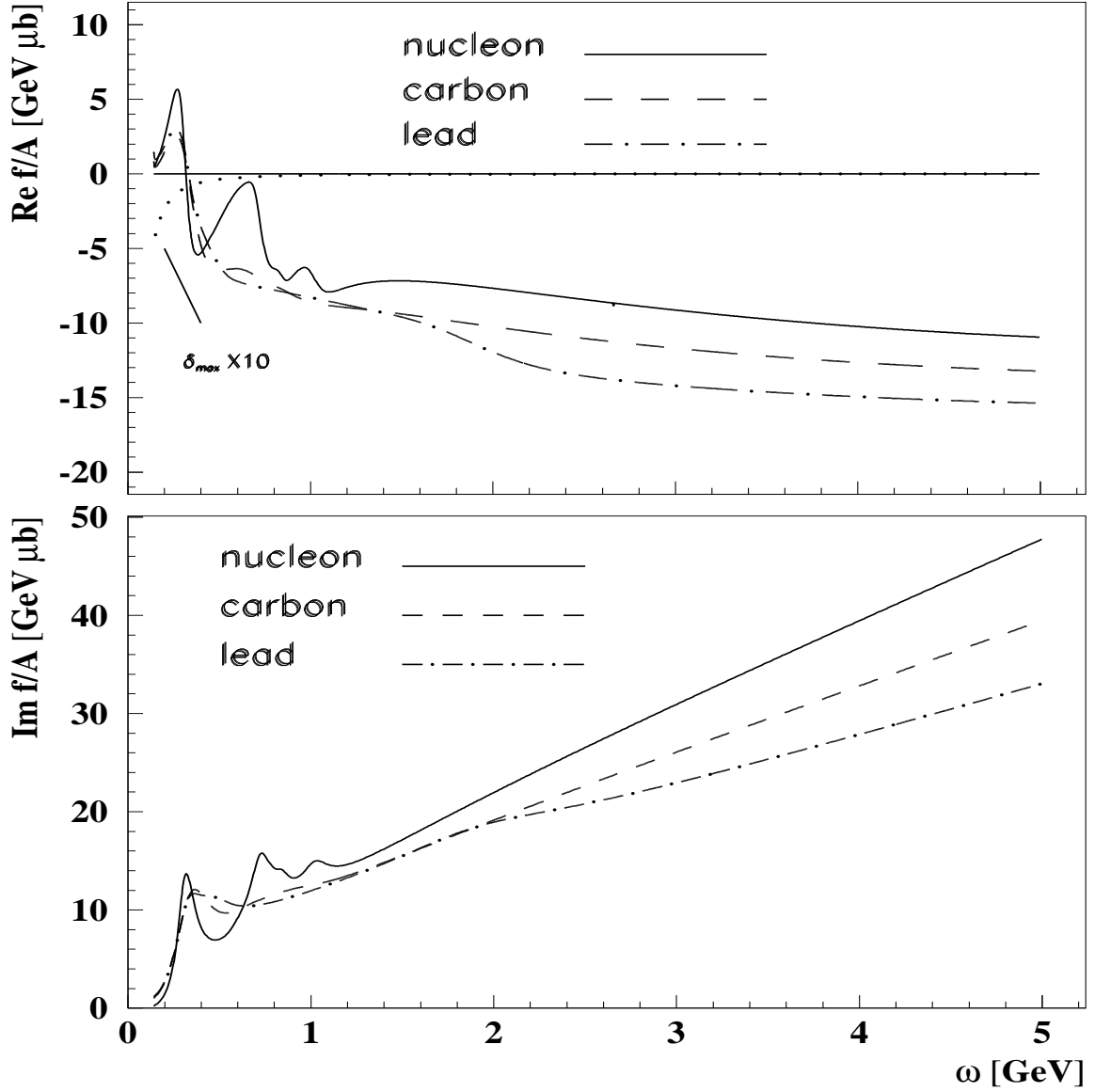
11

Figure 2: The FCA for the given nuclei as a function of the photon energy. The curve for the free-nucleon is calculated from Eq. 2 assuming Z=N=A/2. The dotted line represents the δ_{max} contribution (multiplied by a factor 10) of Eq. (7).

resonance contribution vanishes. This fact may reflect the onset of the shadowing, as suggested in ref. [7].

The energies ω^* at which $Ref(\omega^*) = 0$ (henceforth called zeros of Ref), that correspond to the maximum in the photoabsorption cross sections, give an indication of the Δ-resonance peak positions. For the proton one finds $\omega_p^* = 0.317\pm0.002$ GeV. In the Breit-Wigner parametrization of the Δ-resonance given by Walker et al. [14] this result is in good agreement with the Δ-mass value $M_\Delta = 1.232$ GeV. This finding suggests that, in spite of the presence of a non-resonant background the zero of Ref is a meaningful indication of the Δ-peak position. For carbon and lead one finds $\omega_C^* = 0.328 \pm 0.002$ GeV and $\omega_{Pb}^* = 0.332 \pm 0.002$ GeV. Assuming that the non-resonant contribution is not very different for nuclei as compared to the nucleon, this confirms the increase of the Δ mass inside nuclei suggested in previous analyses [2, 21].

The differences in the FCA for free and bound nucleons are more cleanly seen in the Argand plots shown in Figure 3. While in the free-nucleon curve one sees the loops that reflect the presence of the resonance peaks in the cross section, for carbon and lead there is only the loop corresponding to the Δ-resonance, while those for the high energy resonances disappear. The curve for carbon shows a cusp just after the Δ-loop, at $\omega = 0.525$ GeV corresponding to the minimum in the imaginary part of FCA. Also for lead the main deviation from the free-nucleon behavior starts around 0.525 GeV. This deviation can be ascribed to the different relative strength of the resonance and background contributions in nuclei respect

to the nucleon case, as recently suggested [22, 23].

5 The forward Compton scattering cross section

Using the above determined FCAs, we have calculated the forward Compton scattering cross sections for proton, carbon and lead

$$\frac{d\sigma_{\gamma A \to \gamma A}}{d\Omega}(\theta = 0, \omega) = |f_{\gamma, A}(\omega)|^2 . \tag{20}$$

The results are shown in Figure 4: as can be seen, the difference between bound and free nucleons is enhanced since the nuclear Compton cross section is equal to the sum of the squares of both the real and imaginary parts. The high-mass nucleon-resonances are clearly seen in the proton curve, but are absent in the nuclear ones.

Also shown in the Figure are the available data for proton [24, 25, 26, 27] and carbon [28, 29]. Unfortunately, there are no data for lead and the interesting region of the nucleon-resonances is uncovered by the experiments for carbon. It is worth noticing that proton data at energies between 0.6 and 1.6 GeV are obtained by extrapolating from Compton scattering measurements at relatively high scattering angles ($\Theta_{c.m.} \geq 35$ deg) [24, 25, 26] and then suffer for larger (up to ± 22 %) systematic uncertainties (not shown in Fig. 4), due to the extrapolation
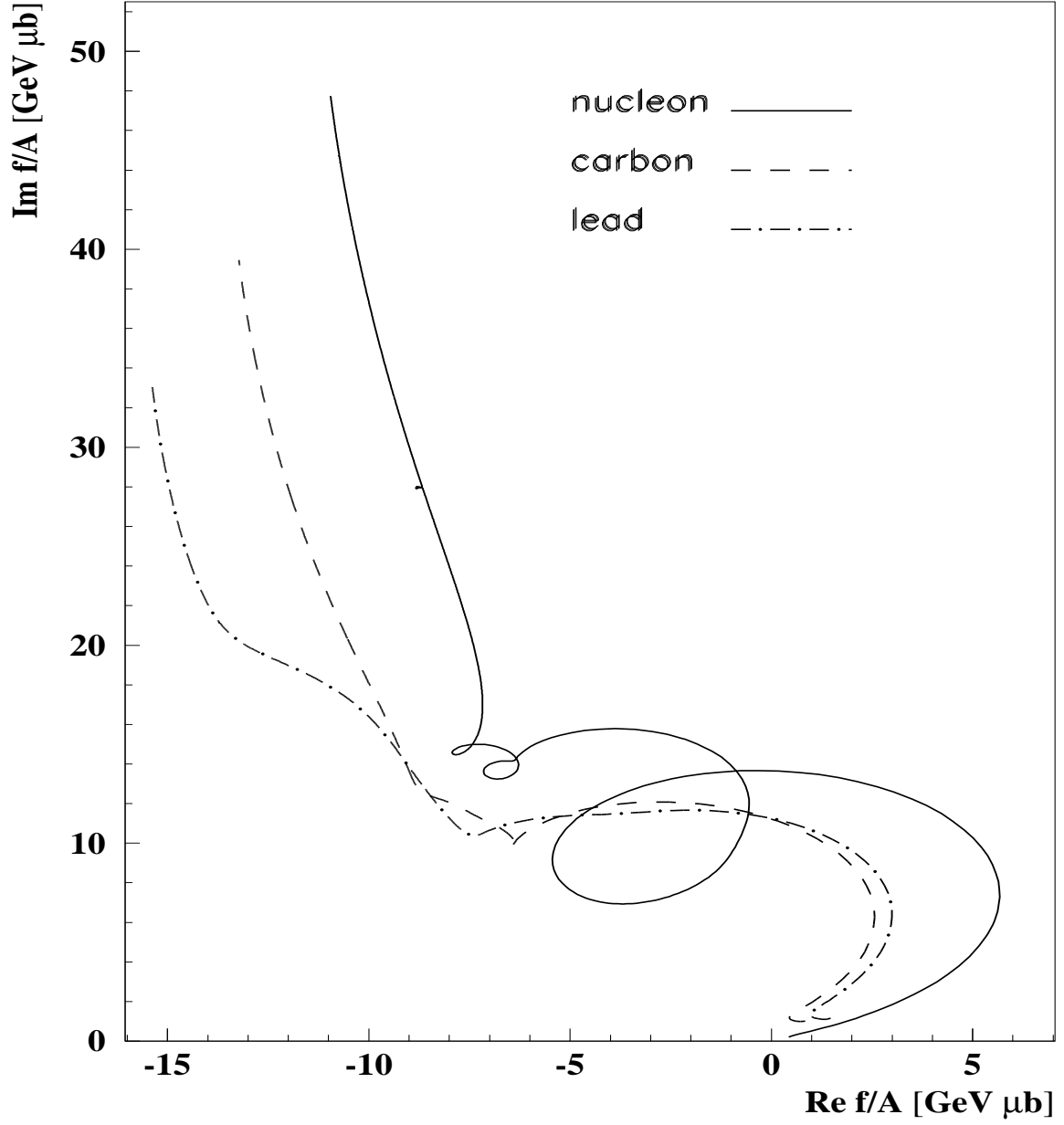
Figure 3: The Argand plot of the FCAs for the given nuclei. The curve for the free-nucleon was calculated assuming Z=N.

procedure. The overall good agreement found between the curves for proton and carbon and the corresponding data demonstrates the reliability of the FCA values calculated with Equations 1 and 4. In addition, this agreement shows the consistency between two complementary sets of data: specifically, the total photoabsorption and the forward Compton scattering data.

This validation of the FCAs is also a verification of the Weise sum rule, which is trivially satisfied by the FCAs calculated here, as can be easily verified by direct substitution of Equation (4) into Equation (8).

The FCA curves are also a useful tool for testing the validity of the models recently proposed to describe the damping of high-mass nucleon-resonances in nuclear medium [22, 30], and the shadowing effect at high energy [5].

As an application, we examine the analysis performed by Boffi et al. [5] who evaluated the quantity $R(\omega)$ of Equation (10) for uranium. In Figure 5 we show their predictions together with our results for carbon and lead. As it is seen the two calculations largely disagree in the whole energy range, and the disagreement is stronger than expected from mass number dependence. In the Δ-region it arises from the less accurate Breit-Wigner parametrization of the nucleon-resonances used by Boffi et al., which results in a shift of the resonance-mass. At higher energies it is due to a not accurate accounting of the shadowing contribution which produces an overestimate of the new photoabsorption data. The disagreement is still larger with the calculation where the two-nucleon correlations are included, which give an antishadowing effect for $\omega < 2$ GeV.
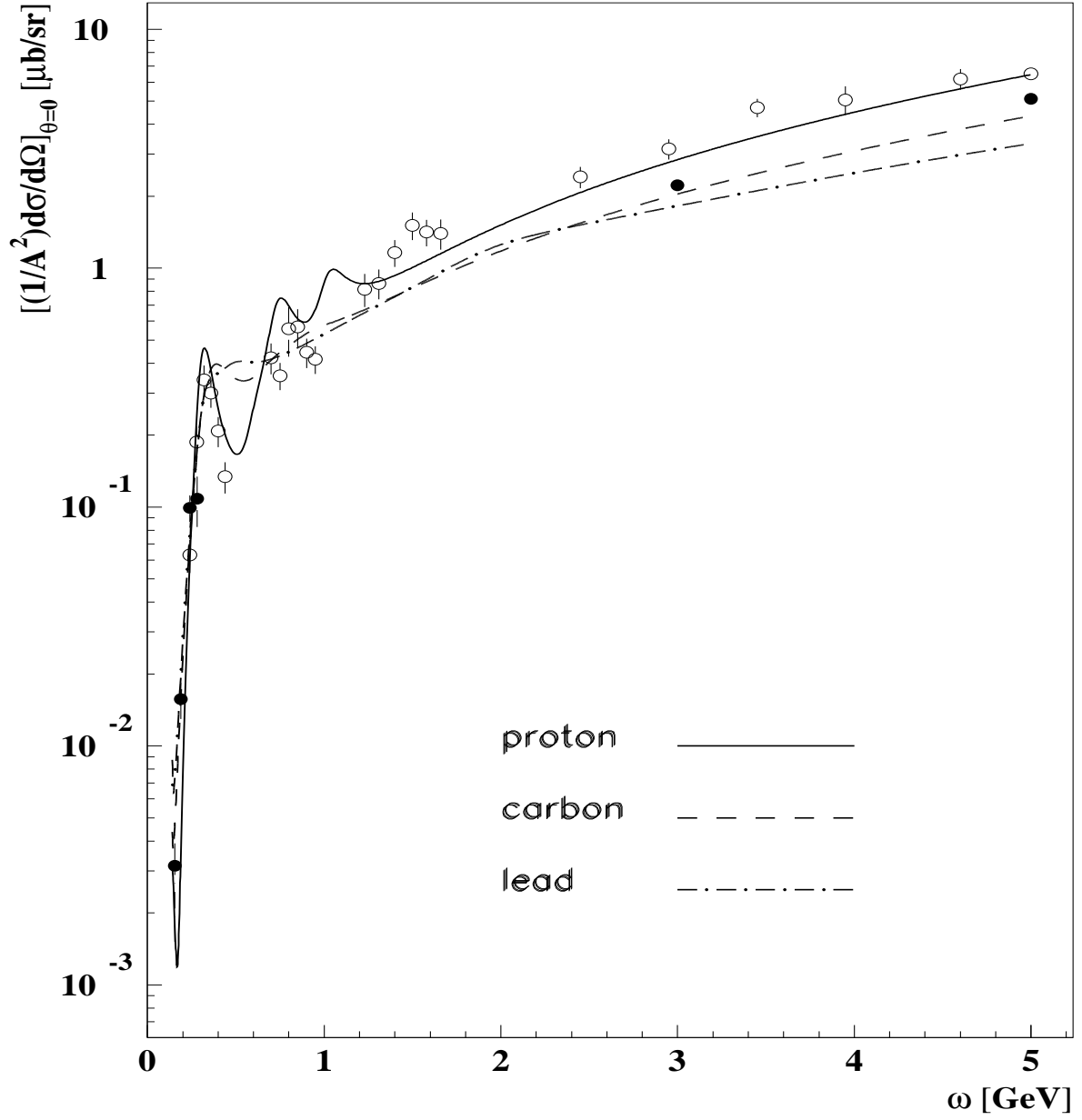
16

Figure 4: Forward Compton scattering differential cross section as calculated with the FCA worked out is this paper. Open and closed circles are data for proton [24, 25, 26, 27] and carbon [28, 29].
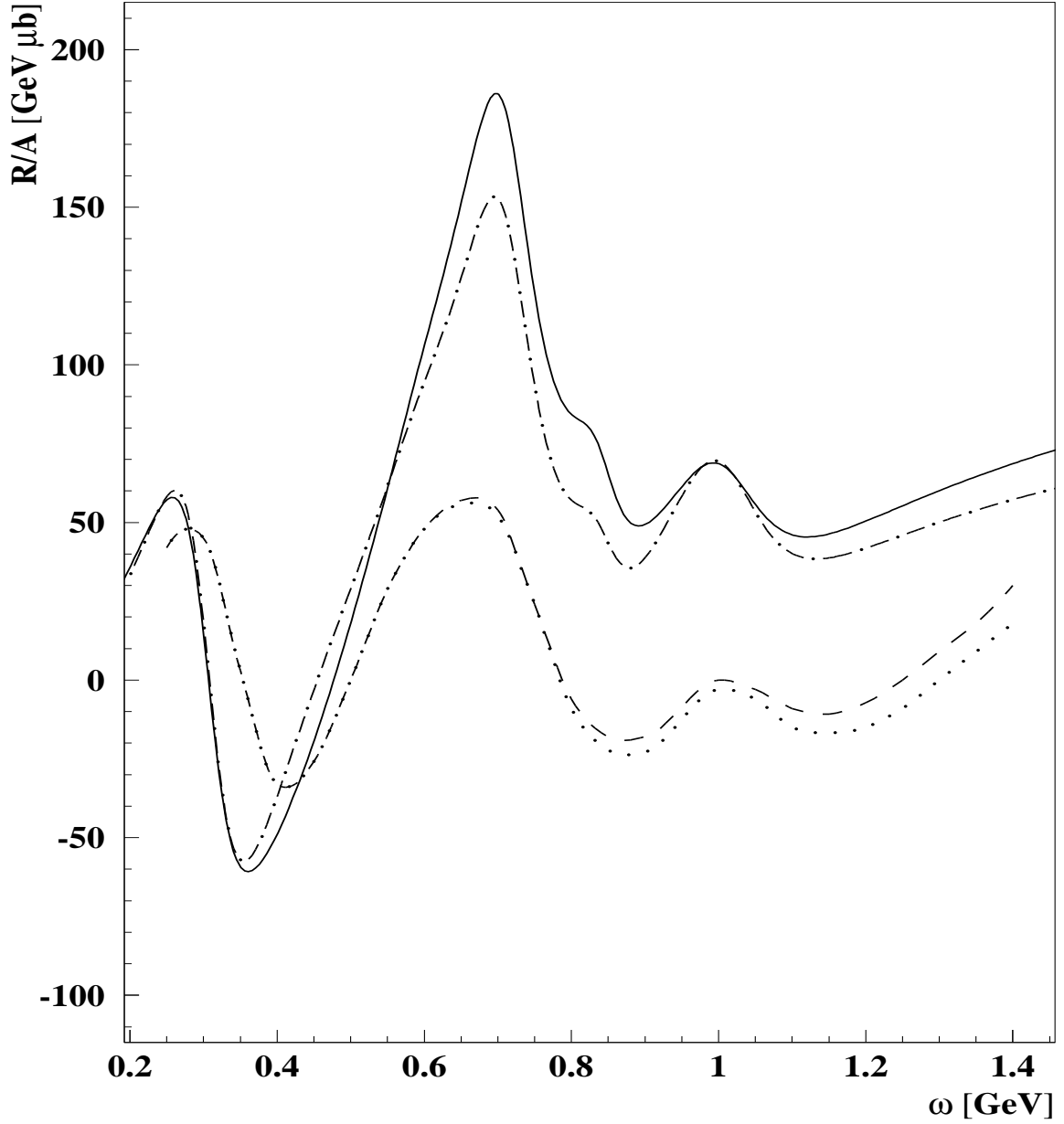
Figure 5: The quantity $R(\omega)$ defined in Equation 10 calculated for lead (solid line) and carbon (dashed-dotted line) is compared with the results for uranium both in the case of correlation (dotted line) and without correlation (dashed line) from reference [5].

6   Conclusion

We have used the data set of the total photoabsorption cross section on carbon and lead, now available in the full range from 0.14 to 80 GeV, to perform an accurate dispersion relation analysis and to determine the forward Compton scattering amplitudes and cross section. The results of this analysis show that

i) in the Δ-resonance region, the FCA curves for the nuclei are similar in shape to the free nucleon ones and the locations of the zero of $Ref_{\gamma A}(\omega)$ suggest a shift of the Δ-resonance mass inside nuclei, in agreement with the conclusions previously drawn from a different analysis [21];

ii) in the high-mass nucleon resonance region, the FCA curves for the nuclei strongly differ from the free-nucleon one. The FCA Argand plots for the nuclei show a sharp deviation from the corresponding curve for the free-nucleon in between of 0.5 - 0.6 GeV, with no signature of high-mass nucleon resonances;

iii) above the nucleon resonance region the reduction of the FCAs for the nuclei may reflect the onset of the shadowing effect;

iv) the forward Compton scattering cross sections derived from the FCAs for carbon and proton are in good agreement with data.

References

[1] J. Ahrens, L. S. Ferreira and W. Weise, Nuc. Phys. A485 (1988) 621.

[2] N. Bianchi et al., Phys. Rev. C54 (1996) 1688

[3] T. Hatsuda and T. Kunihiro, Phys. Report 247 (1994) 221, and reference therein.

[4] N. C. Mukhopadhyay and V. Vento, RPI Internal Report RPI-97,1997-N117.

[5] S. Boffi, Ye. Golubeva, L. A. Kondratyuk and M. I. Krivoruchenko, Nuclear Physics A606 (1996) 421.

[6] W. Weise, Phys. Rev. Lett. (1973) 773 and W. Weise, Phys. Rep . 13 (1974) 53.

[7] M. Mirazita et al., Phys. Lett. B407 (1997) 225.

[8] B. L. Berman, R. Bergère and P. Carlos, Phys. Rev. C26 (1982) 304.

[9] A. Leprètre et al., Nuc. Phys. A367 (1981) 237.

[10] J. Ahrens, Nucl. Phys. A251 (1975) 479.

[11] M. Mac Cormick et al, Phys. Rev. C53, (1996) 41.

[12] Particle Data Group (R.M. Barnett et al.), Phys. Rev. D54, (1996) 191.

[13] The Durham RAL Databases, http://DURPDG.DUR.AC.UK/HEP-DATA.

[14] R. L. Walker et al., Phys. Rev. 182 (1969) 1729.

[15] T. A. Armstrong et al., Phys. Rev. D5 (1972) 1640.

[16] A. Donnachie and P.V. Landshoff, Phys. Lett. B296 (1992) 227.

[17] P. Rossi et al., Phys. Rev. C40 (1989) 2412.

[18] O. A. P. Tavares and M. L. Terranova, J. Phys. G18 (1992) 521.

[19] D. Babusci, G. Giordano and G. Matone, Phys. Rev. C57 (1998) 291.

[20] V. Muccifora Nucl. Phys. A623 (1997) 116c.

[21] S. Boffi, Ye. Golubeva, L. A. Kondratyuk, M. I. Krivoruchenko and E. Perazzi, Phys. of Atomic Nuclei, 60 7 (1997) 1193.

[22] M.M Giannini and E.Santopinto, Phys. Rev. C 49,3 (1994) R1258.

[23] J. A. Gómez Tejedor, M. J. Vicente-Vacas and E. Oset, Nucl. Phys. A588 (1995) 819.

[24] H. Genzel et al., Z. Phys. A279 (1976) 399.

[25] M. Jung et al., Z. Phys. C10 (1981) 197.

[26] J. Duda et al., Z. Phys. C17 (1983) 319.

[27] L. Criegee et al., Nuc. Phys. B121 (1977) 31.

[28] R. Igarashi et al., Phys. Rev. C52 (1995) 755.

[29] L. Criegee et al., Nuc. Phys. B121 (1977) 38.

[30] M. Effenberger et al., Nucl. Phys. A613 (1997) 353.